

Hypoxia induces complex I inhibition and ultrastructural damage by increasing mitochondrial nitric oxide in developing CNS

Sebastián Giusti,¹ Daniela P. Converso,² Juan J. Poderoso² and Sara Fiszer de Plazas¹

¹Institute of Cell Biology and Neuroscience 'Prof. E De Robertis', School of Medicine, University of Buenos Aires, Paraguay 2155, 1121, Buenos Aires, Argentina

²Laboratory of Oxygen Metabolism, University Hospital, University of Buenos Aires, Buenos Aires, Argentina

Keywords: chick optic lobe, complex I, development, hypoxia, mitochondria, mtNOS

Abstract

NO-mediated toxicity contributes to neuronal damage after hypoxia; however, the molecular mechanisms involved are still a matter of controversy. Since mitochondria play a key role in signalling neuronal death, we aimed to determine the role of nitrative stress in hypoxia-induced mitochondrial damage. Therefore, we analysed the biochemical and ultrastructural impairment of these organelles in the optic lobe of chick embryos after *in vivo* hypoxia–reoxygenation. Also, we studied the NO-dependence of damage and examined modulation of mitochondrial nitric oxide synthase (mtNOS) after the hypoxic event. A transient but substantial increase in mtNOS content and activity was observed at 0–2 h posthypoxia, resulting in accumulation of nitrated mitochondrial proteins measured by immunoblotting. However, no variations in nNOS content were observed in the homogenates, suggesting an increased translocation to mitochondria and not a general *de novo* synthesis. In parallel with mtNOS kinetics, mitochondria exhibited prolonged inhibition of maximal complex I activity and ultrastructural phenotypes associated with swelling, namely, fading of cristae, intracristal dilations and membrane disruption. Administration of the selective nNOS inhibitor 7-nitroindazole 20 min before hypoxia prevented complex I inhibition and most ultrastructural damage. In conclusion, we show here for the first time that hypoxia induces NO-dependent complex I inhibition and ultrastructural damage by increasing mitochondrial NO in the developing brain.

Introduction

Evidence indicates that mitochondrial dysfunction, and overproduction of reactive species such as nitric oxide (NO) and superoxide anions (O_2^-), are involved in triggering brain damage after hypoxia–reoxygenation (Volpe, 2001; Won *et al.*, 2002). NO is a highly diffusible free radical synthesized by conversion of L-arginine to L-citrulline via a family of NO synthase (NOS) isozymes. Two isoforms, neuronal NOS (nNOS) and endothelial NOS, are constitutively expressed (Bredt & Snyder, 1990) while a third isoform, inducible NOS, is cytokine-inducible (Forstermann *et al.*, 1992). In the last 10 years, several reports have provided evidence for the existence of mitochondrial NOS (mtNOS) (Giulivi *et al.*, 1998; Tatoyan & Giulivi, 1998). Recently it was characterized as a variant of nNOS α , constitutively localized at the inner membrane with specific post-translational modifications (Elfering *et al.*, 2002).

The finding of an mtNOS led several research groups to explore a possible role for NO in mitochondria. Soon after, it was established that NO elicits changes in free radical production and energy conservation processes (Poderoso *et al.*, 1996). Moreover, under physiological conditions, NO modulates oxygen consumption through the reversible inhibition of cytochrome oxidase (complex IV) (Giulivi, 2003; Haynes *et al.*, 2003).

Reoxygenation after hypoxia or ischemia produces a burst of reactive oxygen species (Sugawara *et al.*, 2004) the main of which, O_2^- , is released into the mitochondrial matrix (Boveris *et al.*, 1976). Under these circumstances and when NO levels are also elevated, deleterious effects of NO-related reactive species, i.e. nitrative stress, may be important.

In a previous study we developed a chick embryo model of normobaric acute hypoxia (Rodriguez Gil *et al.*, 2000). In this model, CO_2 and glucose levels are normal, no invasive procedures to set hypoxia are required and maternal effects are absent. Moreover, in ischemic models it is not possible to distinguish the effects of hypoxia itself from those of hypercapnia and hypoglycaemia. Recently, using the developing chick optic lobe, we have shown that this injury produces at embryonic day (ED)12 an activation of pro-apoptotic proteins followed by an increase in cell death (Pozo Devoto *et al.*, 2006; Vacotto *et al.*, 2006).

Our hypothesis is that cell death in our experimental model is preceded by an overproduction of mitochondrial NO, resulting in mitochondrial damage caused by nitrative stress. Although the role of nitrative stress after a hypoxic injury on developing CNS mitochondria has not been thoroughly studied, two kinds of evidence contributed to the formulation of our hypothesis. First, mtNOS activity increased both in heart mitochondria of rats exposed to hypobaric hypoxia (Zaobornyj *et al.*, 2005) and in liver mitochondria after hypoxia–reoxygenation (Lacza *et al.*, 2001). Second, a powerful oxidizing and nitrating agent formed by the reaction between NO and

Correspondence: Dr Sara Fiszer de Plazas, as above.
E-mail: sfiszer@fmed.uba.ar

Received 13 June 2007, revised 3 October 2007, accepted 15 November 2007

O₂⁻, peroxynitrite (ONOO⁻), reacts with mitochondrial membranes of different tissues, significantly inhibiting the activities of complexes I (Riobo *et al.*, 2001; Murray *et al.*, 2003), II and V (Murray *et al.*, 2003). Despite these findings the information about developing brain and the role of NO in mitochondrial ultrastructural damage is limited.

Using the above mentioned experimental model of prenatal hypoxic brain injury the aims of the present study were to: (i) analyse mtNOS modulation; (ii) investigate mitochondrial functional impairment by assessing electron transfer rate; (iii) characterize mitochondrial ultrastructural changes; and (iv) detect a possible causal relationship between NO production and mitochondrial functional and ultrastructural damage.

Materials and methods

Experimental design

Fertile chicken (*Gallus gallus domesticus*) eggs from White Leghorns were obtained from a local hatchery and incubated at 37 °C and 60% relative humidity. Global hypoxic treatment was induced as previously described (Rodriguez Gil *et al.*, 2000). Briefly, eggs at ED12 were vertically placed in a 10-L plastic chamber inside the incubator (in the same conditions of temperature, pressure and humidity) and subjected to a stream of 8% O₂ and 92% N₂ for 60 min, at a flow rate of 1 L/min. The chamber contained retention valves to allow escape of gases in excess while avoiding mixing with atmospheric air, and a storage space with calcium hydroxide to absorb CO₂ formed during the hypoxic treatment. After normobaric hypoxic treatment, eggs were either returned to their shelves in the incubator for recovery or immediately processed for molecular and biochemical studies. The control consisted of untreated embryos. We focused our analysis on the first 4 h of reoxygenation after hypoxia. When the parameters measured had not returned to control levels within that temporal window, we analysed 24 and 48 h of recovery.

The protocol follows the Guide for the Care and use of Laboratory Animals from the Institute of Laboratory Animals Resources, Commission of Life Sciences, National Research Council, USA (NIH Publication no. 80–23, revised 1996). The number of animals used was minimized accordingly.

NOS inhibition in vivo

On the day prior to hypoxia (ED11) some eggs were windowed following a modification of the Hamburger procedure (Hamburger, 1960). Briefly, a rectangular area of the shell roughly 4–6 mm² in size was removed and the window was covered with Micropore tape (3M). On ED12, 20 min before hypoxia, the tapes were removed and 200 µL of NOS inhibitors or vehicle was applied to the chorioallantoic membrane. Two NOS inhibitors were used: the general NOS inhibitor N^ω-nitro-L-arginine-methyl ester (L-NAME) and the selective nNOS inhibitor 7-nitroindazole (7-NI). Saline and DMSO were their respective vehicles. Three concentrations of inhibitors were used at a final volume of 50 µL per egg: 20, 100 and 500 µM.

Purification of mitochondria

Mitochondria were isolated from chick embryo optic lobes by differential centrifugation, and purified through a discontinuous sucrose gradient as previously described (Rodriguez De Lores Arnaiz & De Robertis, 1962) with minor modifications. Briefly, for each experimental treatment, at least 10 embryos were decapitated and

optic lobes were excised, washed and homogenized (1/3 w/v) in 0.32 M SHE (sucrose, 298 mM; EDTA, 0.5 mM; Tris-HCl, 20 mM; HEPES, 2 mM; leupeptin, 1 µM; aprotinin, 1 µM; pepstatin, 1 µM; and PMSF, 1 µM; pH 7.4) at 4 °C. The homogenate was centrifuged at 600 g for 10 min. The pellet (nuclear fraction) was washed twice by rapid rehomogenization in 0.32 M SHE, at 1/2 w/v and 1/1 w/v of the original tissue weight, respectively, and centrifuged again. The supernatants were pooled and centrifuged at 10 000 g for 20 min. A new supernatant (S2) and a crude mitochondrial pellet were obtained. The latter was redispersed in 0.32 M SHE and carefully layered on the top of the density gradient with 12-mL steps of 0.8 M SHE (sucrose, 778 mM; EDTA, 0.5 mM; Tris-HCl, 20 mM; and HEPES, 2 mM; pH 7.4) and 12 mL of 1.2 M SHE (sucrose, 1178 mM; EDTA, 0.5 mM; Tris-HCl, 20 mM; and HEPES, 2 mM; pH 7.4). The gradients were centrifuged for 2 h at 65 000 g in an SW-28 rotor, separating mitochondria (pellet) from synaptosomes (between 0.8 and 1.2 M). Mitochondria were washed in 20 mL of 0.32 M SHE, centrifuged at 100 000 g for 30 min and resuspended in 0.32 M SHE. Purified mitochondria were tested for contamination by comparing lactate dehydrogenase activity (cytosolic marker) and NADPH-cytochrome c reductase (microsomal marker) to cytochrome oxidase activity (mitochondrial marker); minimal contamination was found (2–5%). Cytosolic fractions were obtained by centrifugation of supernatant S2 at 100 000 g for 30 min. Protein content was assessed as described by Lowry *et al.* (1951) and the samples were stored at –70 °C.

Electron microscopy

Optic lobes were cut into 1–2 mm³ cubes and immersed in cold 2.5% w/v glutaraldehyde (pH 7.2–7.4) dissolved in 0.1 M phosphate buffer for 2 h at 4 °C. Each tissue sample was then postfixed in the same buffer solution supplemented with 1% w/v osmium tetroxide. After two 15-min washes with distilled water, samples were immersed for 2 h in 5% (w/v) uranyl acetate and immediately dehydrated. After embedding in Durcupan, ultrathin sections (70–90 nm) were contrasted with Reynolds' lead citrate (Reynolds, 1963). Micrographs were obtained at 40 000× in a blinded manner by an electron microscopy technician using a C10 Zeiss Electron Microscope and Kodak 5302 films. At least 100 mitochondrial images were analysed in each condition by a blinded investigator. As mitochondria have elliptical shapes, the area occupied by each organelle was calculated by measuring longitudinal and latitudinal radii, r_1 and r_2 , respectively. The area occupied by each mitochondrion was calculated following the formula for the area of an ellipse: $\pi r_1 r_2$.

Western blotting

Total homogenate, cytosolic and mitochondrial fractions were denatured in sodium dodecyl sulphate (SDS)-containing loading buffer (Tris-HCl pH 6.8, 62.5 mM; SDS, 2%; β-mercaptoethanol, 10%; glycerol, 10%; and bromophenol blue, 0.002%) at 100 °C for 10 min and then separated by electrophoresis on an SDS–polyacrylamide gel (Bio-Rad, Richmond, CA, USA) at 7.5% for nNOS or 12% for nitrotyrosine and respiratory complex subunits. Proteins were then transferred to a PVDF membrane (Millipore Corporation, MA, USA). After blocking in 4% milk in phosphate-buffered saline with Tween 20 0.05% in 1× PBS for 1 h, membranes were incubated with the primary antibody overnight at 4 °C followed by HRP-conjugated secondary antibodies (Chemicon International, Inc., CA, USA). For primary antibodies the dilutions used were 1 : 1000 for the anti-nNOS isoform,

monoclonal antibody (N-31020; Transduction Laboratories, Lexington, KY, USA); 1 : 3000 dilution for the anti-3 nitrotyrosine polyclonal antibody; 1 : 5000 dilution for anti-39 kDa Complex I subunit and for anti-8.8 kDa Complex IV subunit monoclonal antibodies (Molecular Probes, AA Leiden, The Netherlands), and 1 : 2000 for anti-mitochondrial transcription factor A (Santa Cruz Biotechnology, Inc). Total homogenate and cytosolic blots were stripped and reprobed for actin (1 : 1000, Chemicon International, Inc., CA, USA) while mitochondrial blots were stripped and reprobed for mitochondrial housekeeping [voltage-dependent anion channel (VDAC); 1 : 1000] to verify equal amounts of protein loading. Bands were detected by chemiluminescence using the ECL Kit (Amersham Pharmacia Biotech). The radioautograms were then scanned and optical density was quantified with Gel-Pro Analyser 3.1.

NOS activity

NOS activity was determined through the conversion of [^3H]-L-arginine to [^3H]-L-citrulline (Knowles & Salter, 1998). The reaction medium consisted of: L-arginine, 100 μM ; L-[2,3- ^3H]-arginine, 0.1 μM (NEN, Boston, MA, USA); NADPH, 0.1 mM; CaCl_2 , 0.3 mM; calmodulin, 0.1 μM ; tetrahydrobiopterin, 10 μM ; flavin adenine dinucleotide, 1 μM ; flavin mononucleotide, 1 μM ; L-valine, 50 mM; and mitochondrial protein, 0.1 mg in 50 mM of potassium phosphate buffer (pH 7.5). Specific activity was calculated by subtracting the remaining activity in the presence of 10-fold excess concentration of the NOS inhibitor N^G -methyl-L-arginine.

Enzymatic marker activities

Mitochondrial enzymatic activities were determined at 30 °C using mitochondrial fractions at 0.1 mg protein/mL in a Hitachi U3000 spectrophotometer.

Complex I (NADH: ubiquinone oxidoreductase) activity was determined by monitoring the reduction of 0.1 mM NADH with a molar absorption coefficient (ϵ) at 340 nm = $6.81 \text{ mM}^{-1}\text{cm}^{-1}$, using 10 μM benzoquinone as an electron acceptor. Reactions were carried out in the presence of 1 mM KCN. Complex I was selectively inhibited by 1 μM rotenone. Results were expressed as nmoles of oxidized NADH per min per mg protein or as a percentage of control activity.

Complex IV (cytochrome oxidase) activity was determined by recording the oxidation of 50 μM reduced cytochrome c at 550 nm ($\epsilon_{550} = 21 \text{ mM}^{-1}\text{cm}^{-1}$). The rate of the reaction was determined as the pseudo-first-order reaction constant, k' , and expressed per min per mg protein or as a percentage of control activity.

Data analysis

Goodness-of-fit (χ^2 test) was used to compare the frequencies of ultrastructural damage. One-way ANOVA and Dunnett's post-test were used to compare optical densities in Western blot experiments, average area occupied by mitochondria and enzymatic activities. Statistical significance was accepted when $P < 0.05$.

Results

Ultrastructural changes in brain mitochondria

Typical control brain mitochondria showed well-defined cristae and membrane integrity. The main indicators of mitochondrial ultrastructural damage in our system were strongly associated with mitochon-

drial swelling: electron-lucent matrix with poorly-defined cristae, intracristal dilation and membrane disruption (Fig. 1a).

We observed herein an acute period of damage in the first 2 h of reoxygenation as demonstrated by a coincidence of highest values of all the three parameters of injury (Fig. 1b). Accordingly, the average area occupied by each mitochondrion, an indicator of swelling, was found to be significantly increased during the same period (Table 1). Late reoxygenation, i.e. 24 and 48 h after hypoxia, showed no differences when compared to matched controls.

Reversal of mitochondrial damage was likewise due to loss of affected cells and not to an increase in mitochondrial biogenesis; Western blot of cytosol and mitochondrial fractions did not reveal variations in mTFA, a marker of mitochondrial biogenesis, up to 48 h after the start of reoxygenation (data not shown).

Increase in mtNOS correlated with NO production and nitrative stress in mitochondria

Immunoblots of homogenate and cytosolic fractions with specific antibodies did not reveal substantial variations in nNOS α with respect to control values up to 4 h after the start of reoxygenation (Fig. 2a and b). In contrast, mitochondrial fractions showed a transient but substantial increase in mtNOS content at the end of the hypoxic period which lasted for the first 2 h of reoxygenation (Fig. 2c). Accordingly, the NOS-dependent NO production rate increased in the mitochondrial fraction with the same temporal profile (Fig. 2e).

In this context, when using an anti-3 nitrotyrosine antibody we detected an increase in nitrated mitochondrial proteins, a biomarker of nitrative stress, following the temporal distribution of mtNOS expression and activity (Fig. 3) and clearly above the background tyrosine nitration of freshly isolated mitochondria at equal protein loading.

mtNOS protein content and mitochondrial protein tyrosine nitration remained within control values during late reoxygenation and up to the end of the experiment (Figs 2d and 3d).

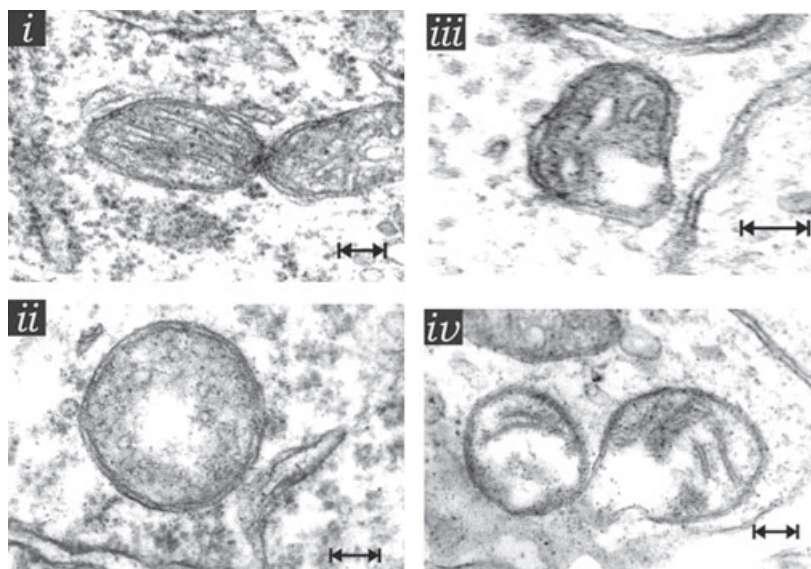
Inhibition of respiratory complexes

Mitochondrial electron transfer rate was assessed by measuring maximal activities of complex I (NADH: ubiquinone oxidoreductase) and complex IV (cytochrome c oxidase) in mitochondrial fractions. Under control conditions, we observed no variation in maximal activities of either complex during the embryonic days studied. The average value for complex I was 12.75 ± 0.48 nmoles of oxidized NADH per min per mg protein, and k' for complex IV was 8.15 ± 0.67 per min per mg protein ($n = 4$). Hypoxia-reoxygenation did not affect complex IV maximal activity at any time point analysed (Fig. 4b). Instead, complex I activity remained significantly inhibited at the end of hypoxia and recovered to control values after 48 h of reoxygenation (Fig. 4a). Immunoblots of mitochondrial fractions using antibodies against a 39-kDa subunit of complex I and an 8.8-kDa subunit of complex IV showed no variations among experimental treatments, arguing against variations in the expression of the complexes (Fig. 4c).

NO-dependence of complex I inhibition and ultrastructural damage

In ovo administration of the nNOS inhibitor 7-NI 20 min prior to hypoxia prevented complex I inhibition in a dose-dependent manner (Fig. 5). 7-NI also prevented intracristal dilation and membrane

(a)



(b)

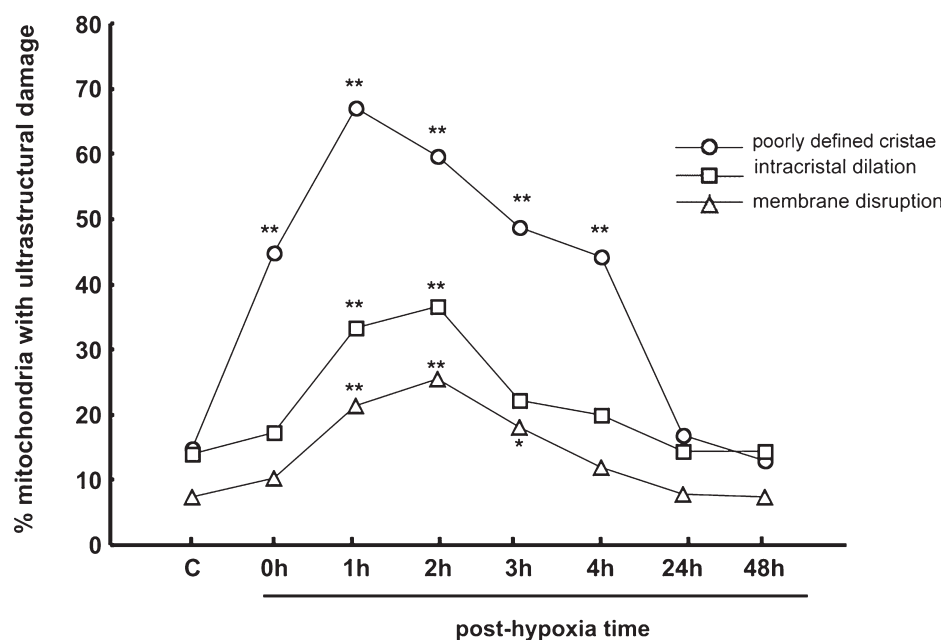


FIG. 1. Hypoxia–reoxygenation induced ultrastructural changes in brain mitochondria. (a) Electron micrographs of brain mitochondria. (i) Typical control mitochondria showing conserved structure and well-defined cristae. (ii) Poorly-defined cristae, (iii) intracristal dilations and (iv) membrane rupture are the major ultrastructural changes observed in mitochondria after hypoxia–reoxygenation. (b) Time course of ultrastructural damage frequencies. At least 100 mitochondria were analysed in each condition. Significantly different from ED-matched control value (* $P < 0.05$ or ** $P < 0.01$, goodness-of-fit, χ^2 test). Scale bar, 100 nm.

disruption but had little effect on cristae definition (Fig. 6). Similar results were obtained with the general NOS inhibitor L-NAME, although it was less effective at the same concentration (Figs 5 and 6).

These results confirm that complex I inhibition and ultrastructural damage after hypoxia–reoxygenation are mediated, at least in part, by

NO. Effect of NOS inhibitors on complex I inhibition and on ultrastructural damage were assayed at the time points in which those injuries were maximal: 1 and 2 h posthypoxia, respectively.

As mitochondrial protein nitration had returned to control levels at 24 h, we analysed the effect of 7-NI at this time point to control for

TABLE 1. Area occupied by each mitochondrion

Treatment	Area ($\times 10^4 \text{ nm}^2$)
Control ED 12	4.64 \pm 0.35
Control ED 13	5.12 \pm 0.39
Control ED 14	4.54 \pm 0.41
Post-hypoxia time	
0 h	5.53 \pm 0.45
1 h	10.86 \pm 2.85**
2 h	10.05 \pm 1.04*
3 h	7.87 \pm 0.80
4 h	6.63 \pm 0.64
24 h (ED 13)	5.04 \pm 0.36
48 h (ED 14)	4.94 \pm 0.38

At least 100 mitochondria were analysed in each condition. ED, embryonic day. Values are means \pm SEM. * P < 0.05, ** P < 0.01 vs. ED-matched control value (ANOVA and Dunnett's post-test).

any effect of other agents distinct from NO in the remaining complex I inhibition. All the concentrations tested prevented the inhibition of this enzymatic activity (data not shown).

Discussion

This paper shows, for the first time, that brain mitochondria increase mtNOS content and activity, and exhibit NO-dependent ultrastructural damage and reversible inhibition of complex I, after *in vivo* prenatal hypoxia-reoxygenation. The sequence of events leading to transient mitochondrial damage includes: (i) a brief mtNOS peak; (ii) transient nitration of mitochondrial proteins; (iii) prolonged blockade of electron transfer at mitochondrial complex I; and (iv) recovery 1–2 days after insult. Reversal of mitochondrial hypoxic damage is likewise due to: (i) a new mitochondrial population, achieved by replacement of affected cells; (ii) an increase in mitochondrial

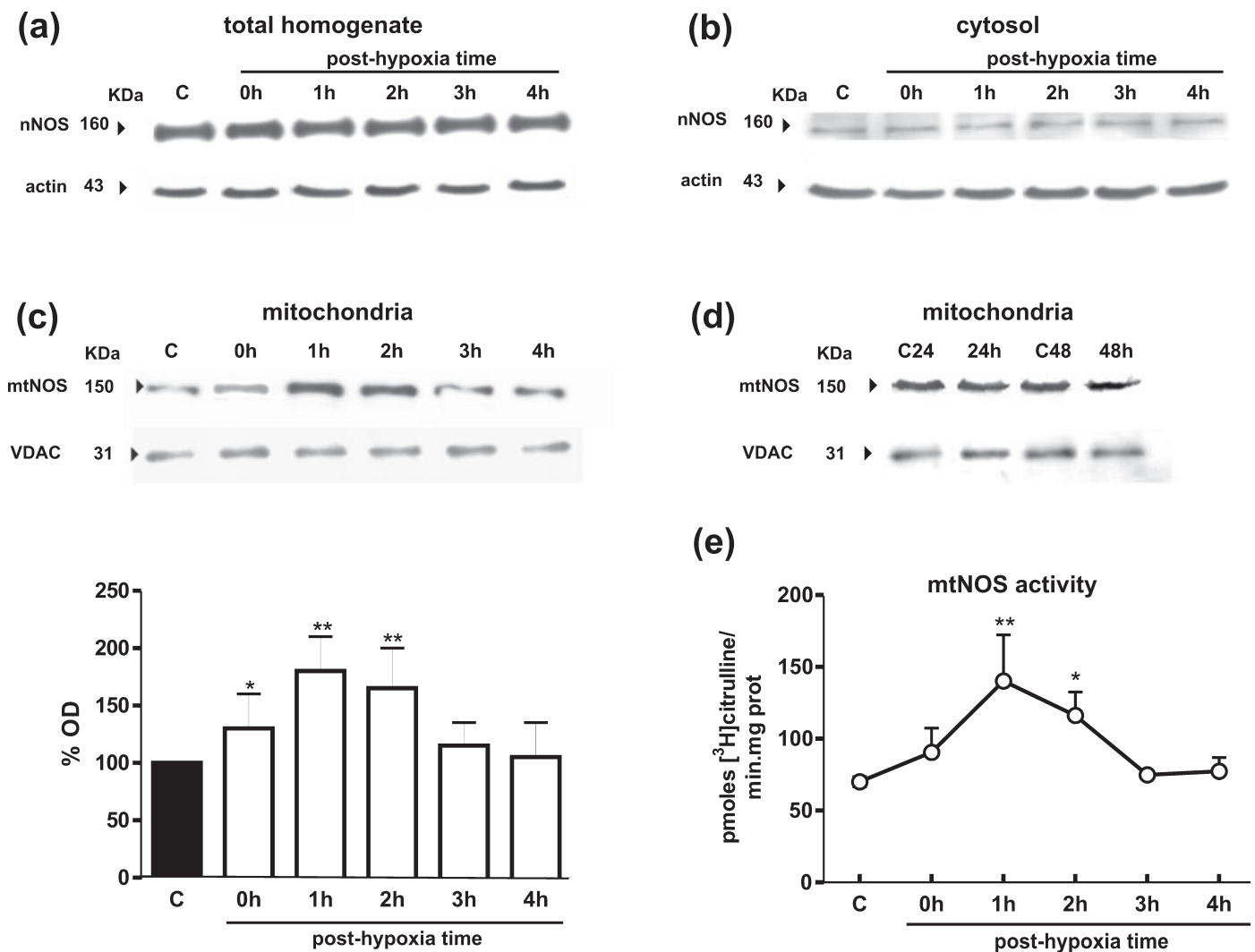


FIG. 2. Hypoxia-reoxygenation increased mtNOS expression but not total or cytosolic nNOS. Representative immunoblotting of (a) homogenates and (b) cytosolic fractions revealed with anti-nNOS antibody. Membranes were stripped and reprobed with antiactin to confirm equal protein loading. (c and d) Representative immunoblotting of mitochondrial fractions revealed with anti-nNOS antibody, and (c) densitometric analysis of 0–4 h kinetics. Equal protein loading in mitochondrial fractions was assessed with an antibody against the constitutive mitochondrial protein VDAC (voltage-dependent anion channel). (e) mtNOS activity in mitochondrial fractions measured by the conversion of [^3H]-L-arginine to [^3H]-L-citrulline. Values are means \pm SEM of $n = 4$ independent experiments. * P < 0.05, ** P < 0.01 vs. control value (ANOVA and Dunnett's post-test).

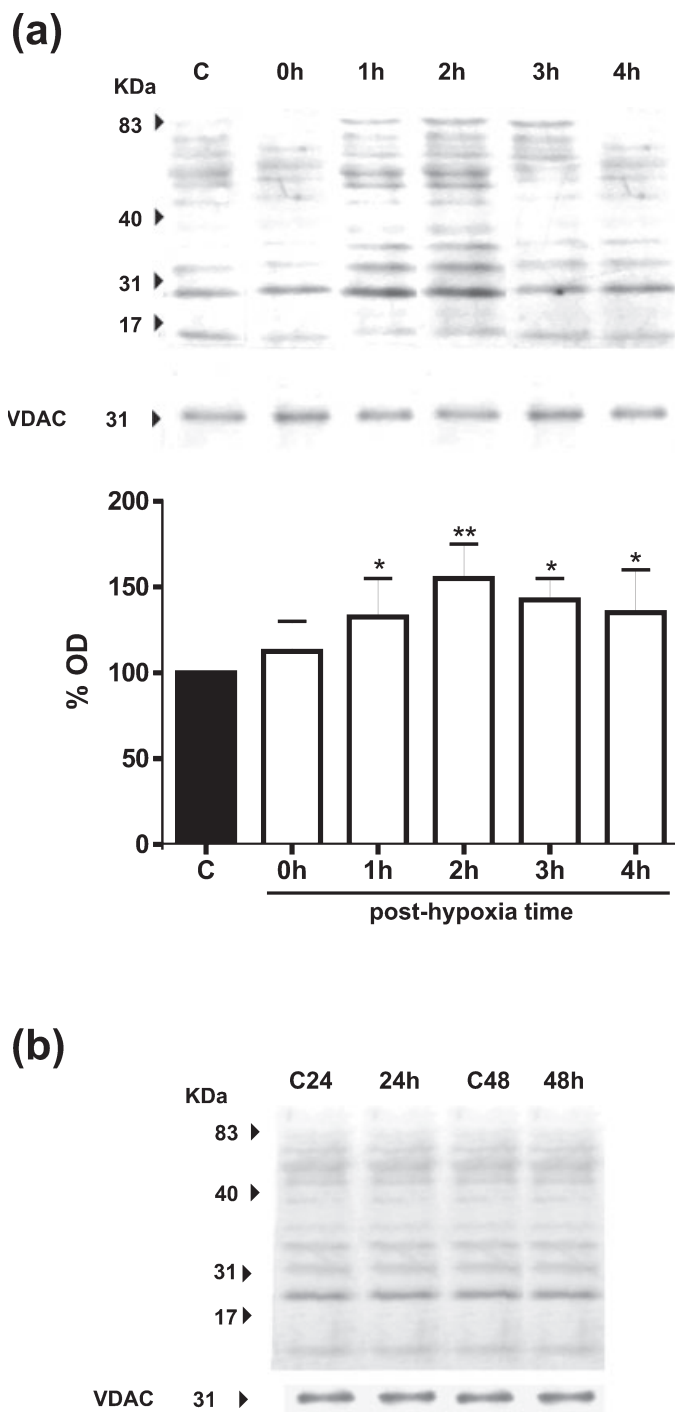


FIG. 3. Hypoxia–reoxygenation increased nitrated mitochondrial proteins. Representative immunoblotting of mitochondrial fractions revealed with anti-3-nitrotyrosine antibody treatments in late reoxygenation at (a) early and (b) late reoxygenation. Densitometric analysis of 0–4 h kinetics is included. The same analysis showed no differences among treatments during late reoxygenation. All-lane optical density was measured. Membranes were stripped and reprobed with anti-VDAC to confirm equal protein loading. Optical density values are means \pm SEM of $n = 4$ independent experiments. * $P < 0.05$, ** $P < 0.01$ vs. control value (ANOVA and Dunnett's post-test).

biogenesis; or (iii) protein denitration. It is suggested that the first option as more probable, considering that Western blot of cytosol and mitochondrial fractions did not reveal variations in mTFA, a marker of mitochondrial biogenesis, up to 48 h after the start of reoxygenation

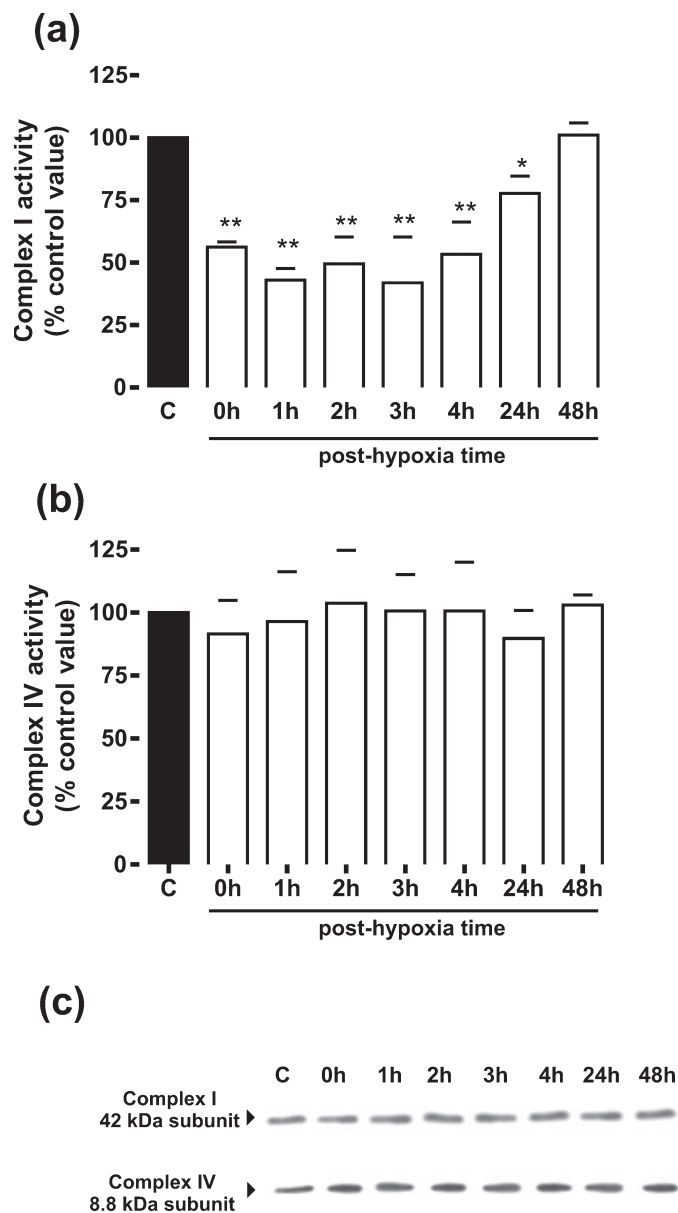


FIG. 4. Effect of hypoxia–reoxygenation on mitochondrial enzyme activities. (a) Complex I and (b) complex IV maximal activities expressed as percentages of control values. Values are means \pm SEM of $n = 4$ independent experiments. * $P < 0.05$ or ** $P < 0.01$ vs. control value (ANOVA and Dunnett's post-test). (c) Immunoblotting with antibodies against a subunit of each complex. Densitometric analysis showed no differences among treatments (data not shown).

(data not shown) and denitration requires specific enzymes not described in chicken embryos.

The mechanism of mtNOS activation is not yet defined. In previous studies, we and others found modulation of mtNOS by thyroid hormones (Carreras *et al.*, 2001) and exposure to cold (Peralta *et al.*, 2003). Of particular significance are calcium stimuli: an increase in cell calcium increases mtNOS activity (Ghafourifar *et al.*, 1999). Considering that hypoxia stimulates mtNOS and calcium influx, the putative connection between the two effects needs to be further explored. Moreover, activation of NMDA receptors during hypoxia may trigger Ca^{2+} increase and mtNOS activation.

Based on previous results indicating the reversible inhibition of cytochrome oxidase by NO, recent studies support a relevant role for

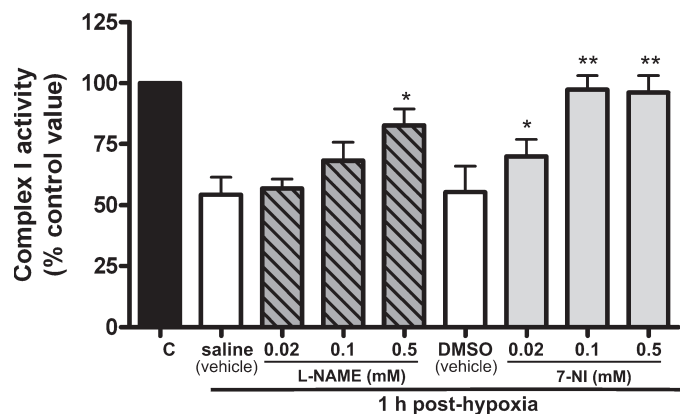


FIG. 5. Effect of *in vivo* administration of NOS inhibitors on hypoxia-reoxygenation induced complex I inhibition. Embryos were injected 20 min before hypoxia with L-NAME, 7-NI or their respective vehicles, saline or DMSO. Controls were injected with vehicle. Complex I maximal activities were measured 1 h posthypoxia and expressed as percentages of control value. Values are means \pm SEM of $n = 4$ independent experiments. * $P < 0.05$ or ** $P < 0.01$ vs. vehicle-treated 1 h posthypoxia value (ANOVA and Dunnett's post-test).

mtNOS in mitochondrial physiology controlling oxygen consumption (Franco *et al.*, 2006; Giulivi *et al.*, 2006). As a negative regulator for mitochondrial respiration, mtNOS allows enough ATP production while it prevents the occurrence of anoxic foci and thus facilitates the redistribution of oxygen within the cell. A high Ca^{2+} concentration and translocation of NOS to mitochondria would be expected to regulate this effect. In this context the study of mtNOS content and activity after a hypoxic insult becomes highly relevant. It has been reported that mtNOS activity increases after hypoxia in isolated liver mitochondria (Schild *et al.*, 2003) and after sustained hypobaric hypoxia in young rat hearts (Zaobornyj *et al.*, 2005). The effect of *in vivo* hypoxia-reoxygenation on mtNOS has been previously studied in adult mice using liver preparations (Lacza *et al.*, 2001), in which mtNOS activity was found to be up-regulated 6 h posthypoxia but no changes were detected in protein content as measured by immunoblotting. However, no information about the effect of hypoxia-reoxygenation on mtNOS expression and activity in brain is yet available. In the present study a transient increase in mtNOS content and activity was observed at 0–2 h posthypoxia (Fig. 2c and d). Our results suggest an increased translocation of nNOS to mitochondria and not a general *de novo* synthesis, as no variations were observed in the homogenates (Fig. 2a). This translocation was not reflected in a decrease in the optical density of the immunoblots of homogenates and cytosolic fractions (Fig. 2b) due to the high concentration of nNOS found in these fractions when compared to the mitochondrial one.

Inhibition of mtNOS by different NOS inhibitors impedes the NO burst in mitochondria and the sequential progression of the cohort of damaging events. Complete protection was particularly observed with 7-NI. Many years ago we demonstrated that high-dose 7-NI almost totally abolished mtNOS activity (Carreras *et al.*, 2002). 7-NI was applied to the chorioallantoic membrane, which is highly vascularized and allows a rapid uptake of molecules into the embryonic circulation and diffusion through the immature blood–brain barrier (Ribatti *et al.*, 1993). Moreover, 7-NI diffuses well in neural tissues and brain (Bush & Pollack, 2001).

During reoxygenation after hypoxia–ischemia there is a surge of superoxide anions (O_2^-) produced by the leaking of electrons from various respiratory complexes to molecular oxygen (Cadenas *et al.*,

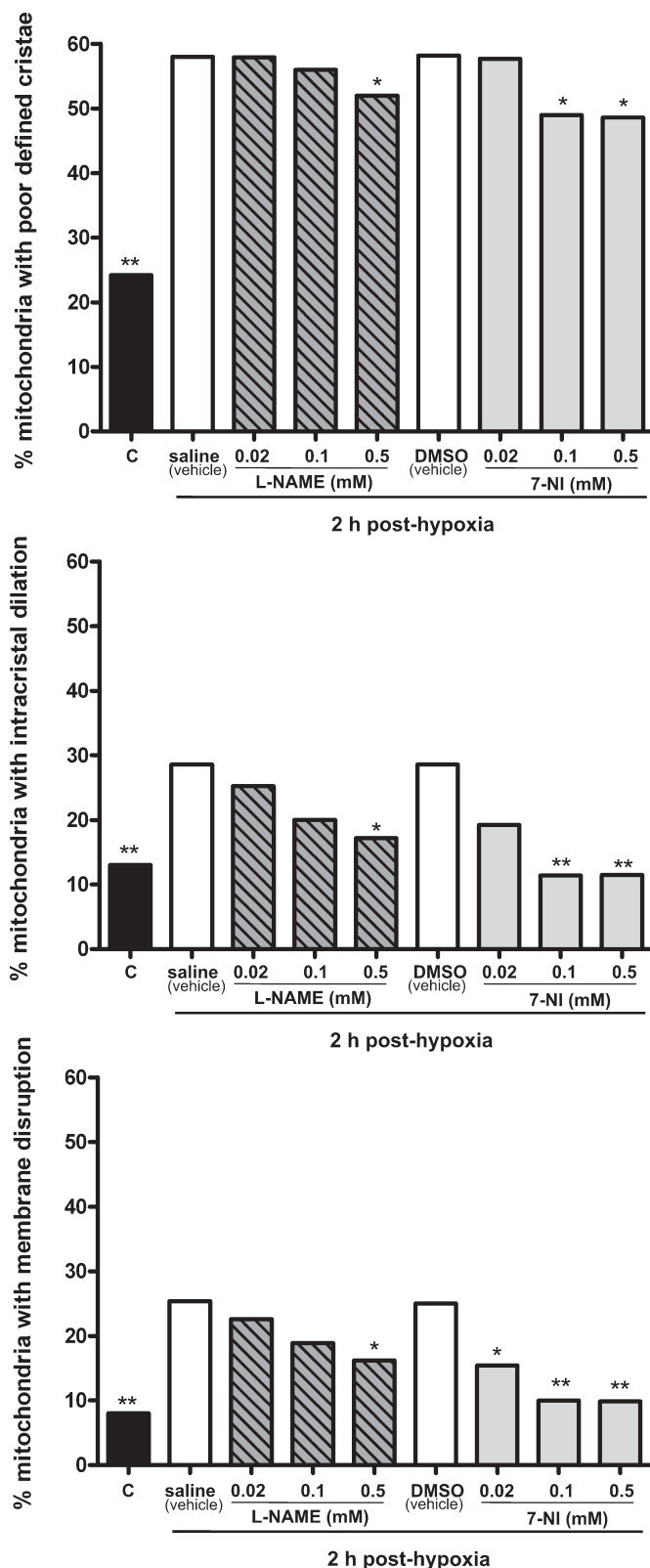


FIG. 6. Effect of *in vivo* administration of NOS inhibitors on hypoxia-reoxygenation-induced mitochondrial ultrastructural changes. Embryos were injected 20 min before hypoxia with L-NAME, 7-NI or their respective vehicles, saline or DMSO. Controls were injected with vehicle. Ultrastructural damage frequencies of at least 100 mitochondria were analysed in each condition. * $P < 0.05$ or ** $P < 0.01$ vs. vehicle-treated 2 h posthypoxia value (goodness-of-fit, χ^2 test).

1977; Turrens & Boveris, 1980; Han *et al.*, 2001). These reactions are strongly favoured by the large concentration of reduced components of the electron transport chain. Furthermore, an increase in mitochondrial NO concentration is compatible with the observed mtNOS translocation. It has also been reported that Ca^{2+} , the main regulator of mtNOS activity, accumulates in mitochondria during hypoxia (Puka-Sundvall *et al.*, 2000a; Solien *et al.*, 2005). However, as NO is a diffusible gas, cytosolic NOS activity may also contribute to an increase in NO in mitochondria. The simultaneous increase in NO and O_2^- levels lead to a stoichiometric overproduction of peroxynitrite (ONOO^-) and related molecules. ONOO^- overproduction has been implicated in neuronal ischemic damage (Eliasson *et al.*, 1999) and is consistent with the accumulation of nitrated mitochondrial protein observed in this study (Fig. 3), as tyrosine nitration is mediated by ONOO^- and other reactive nitrogen species formed as secondary products of NO metabolism in the presence of oxidants (Radi, 2004). Previous reports have provided immunoreactivity-based morphological and biochemical evidence of enhanced nitrotyrosine formation after hypoxia–ischemia in neonatal rat brain (Hattori *et al.*, 2002; Zhu *et al.*, 2004). In line with those studies, isolated mitochondria subjected to hypoxia, in an *in vitro* model, have shown increased tyrosine nitration in the reoxygenation period (Koeck *et al.*, 2004).

Here we also show that, unlike complex IV, mitochondrial respiratory complex I (NADH: ubiquinone oxidoreductase) presents an inhibition of its maximal activity ($\sim 45\%$) following the temporal distribution of mtNOS induction and abundance of nitrated mitochondrial proteins (Fig. 4). We demonstrate, for the first time, the NO-dependence of that dysfunction as this was prevented in a dose-dependent manner by the selective nNOS inhibitor 7-NI (Fig. 5). This observation contributes to linking two kinds of evidence: (i) hypoxia provokes an impairment of mitochondrial respiration (Puka-Sundvall *et al.*, 2000b; Clarkson *et al.*, 2007); and (ii) the specific inhibitory effects of NO and peroxynitrite on complex I in three experimental models: complex I-enriched preparations (Pearce *et al.*, 2005), isolated mitochondrial membranes (Riobo *et al.*, 2001; Murray *et al.*, 2003) and cultured neurons (Yamamoto *et al.*, 2002; Araujo *et al.*, 2004). Complex I is formed by >40 different peptide subunits, a noncovalently bound flavin, heme groups and a series of iron–sulphur clusters (Carroll *et al.*, 2003). Several mechanisms have been suggested for explaining NO-dependent inhibition of this complex. One of them, with strong support in the literature, is the tyrosine nitration of peptide subunits. In fact, immunological and mass spectrometric approaches coupled with two-dimensional PAGE revealed that five subunits of complex I had a 3-nitrotyrosine signature after incubation of mitochondria with ONOO^- (Murray *et al.*, 2003). This was confirmed by the finding of nitrated subunits in other studies on complex I inhibition (Yamamoto *et al.*, 2002; Pearce *et al.*, 2005). Furthermore, Pearce *et al.* (2005) carefully examined the effects of NO and ONOO^- on the cofactors of isolated complex I and found that none of the hemes, iron–sulphur clusters or flavin were affected to any measurable extent. Therefore, NO-dependent inhibition of complex I observed in our study might be associated with tyrosine nitration of peptide subunits.

Our result showing lack of irreversible inhibition on complex IV is consistent with previous studies showing that NO reversibly inhibits this complex (Giulivi, 2003; Haynes *et al.*, 2003).

We also report for the first time that hypoxia–reoxygenation alone induces ultrastructural changes that are compatible with mitochondrial swelling (Fig. 1), peaking at the same time as nitrative stress indicators. These changes might be related to the occurrence of mitochondrial permeability transition (MPT) in the immature brain, as

it has been demonstrated that MPT can be induced when mitochondria accumulate large amounts of calcium and/or are exposed to oxidative stress, collapsing the mitochondrial membrane potential ($\Delta\Psi$) and dissipating proton and ion gradients (Zoratti & Szabo, 1995). We have shown that the mitochondrial ultrastructural damage observed in our model is at least in part NO-dependent as intracristal dilation and membrane disruption could be prevented by 7-NI and L-NAME administration (Fig. 6). However, cristae remained poorly defined, reflecting the fact that this is the most sensitive parameter and that another damaging factor, e.g. reactive oxygen species, might be acting.

In conclusion, we show here that, after the hypoxic insult, the developing brain exhibits NO-dependent mitochondrial ultrastructural damage and prolonged inhibition of complex I, in correlation with mtNOS induction. In addition to the specific increase in mitochondrial NO production described above, results from another group, based on the diffusion of this gas, support the assumption that mitochondrial-generated NO decays within the organelle (Kanai *et al.*, 2001). Moreover, NO produced by mtNOS tends to concentrate in the nonpolar milieu of the inner mitochondrial membrane due to its hydrophobicity (Goss *et al.*, 1999). Thus, it seems likely that the nitrative stress observed is mainly caused by mtNOS-produced NO, although we cannot discount the contribution of cytosolic NO derived from nNOS because specific nNOS vs. mtNOS inhibitors have not yet been developed.

As mitochondria have a pivotal role in apoptotic signalling, the mitochondrial changes described in this study might be upstream in the molecular events leading to cell death in our model (Vacotto *et al.*, 2006). The understanding of the molecular pathways of mitochondrial damage induced by hypoxia–reoxygenation will be important for the development of rational therapeutic approaches.

Acknowledgements

This research was supported by grants from University of Buenos Aires (M028 and M063), National Research Council (PIP5410), the National Agency for Promotion of Scientific and Technological Development (PICT 8468 and PICT 38234) and The Fundación Perez Companc, Buenos Aires Argentina. 3-Nitrotyrosine antibodies were a kind gift from Dr Alvaro Estevez. The authors gratefully acknowledge the expert technical assistance of Mrs Mariana López Ravasio.

Abbreviations

7-NI, 7-nitroindazole; ED, embryonic day; L-NAME, N^G -nitro-L-arginine-methyl ester; mtNOS, mitochondrial NOS; nNOS, neuronal NOS; NO, nitric oxide; NOS, NO synthase; O_2^- , superoxide anion; ONOO^- , peroxynitrite anion; VDAC, voltage-dependent anion channel.

References

- Araujo, I.M., Verdasca, M.J., Ambrosio, A.F. & Carvalho, C.M. (2004) Nitric oxide inhibits complex I following AMPA receptor activation via peroxynitrite. *Neuroreport*, **15**, 2007–2011.
- Boveris, A., Cadenas, E. & Stoppani, A.O. (1976) Role of ubiquinone in the mitochondrial generation of hydrogen peroxide. *Biochem. J.*, **156**, 435–444.
- Bredt, D.S. & Snyder, S.H. (1990) Isolation of nitric oxide synthetase, a calmodulin-requiring enzyme. *Proc. Natl Acad. Sci. USA*, **87**, 682–685.
- Bush, M.A. & Pollack, G.M. (2001) Pharmacokinetics and pharmacodynamics of 7-nitroindazole, a selective nitric oxide synthase inhibitor, in the rat hippocampus. *Pharm. Res.*, **18**, 1607–1612.
- Cadenas, E., Boveris, A., Ragan, C.I. & Stoppani, A.O. (1977) Production of superoxide radicals and hydrogen peroxide by NADH-ubiquinone reductase and ubiquinol-cytochrome c reductase from beef-heart mitochondria. *Arch. Biochem. Biophys.*, **180**, 248–257.

- Carreras, M.C., Melani, M., Riobo, N., Converso, D.P., Gatto, E.M. & Poderoso, J.J. (2002) Neuronal nitric oxide synthases in brain and extraneuronal tissues. *Meth. Enzymol.*, **359**, 413–423.
- Carreras, M.C., Peralta, J.G., Converso, D.P., Finocchietto, P.V., Rebagliati, I., Zaninovich, A.A. & Poderoso, J.J. (2001) Modulation of liver mitochondrial NOS is implicated in thyroid-dependent regulation of O₂ uptake. *Am. J. Physiol. Heart Circ. Physiol.*, **281**, H2282–H2288.
- Carroll, J., Fearnley, I.M., Shannon, R.J., Hirst, J. & Walker, J.E. (2003) Analysis of the subunit composition of complex I from bovine heart mitochondria. *Mol. Cell Proteomics*, **2**, 117–126.
- Clarkson, A.N., Clarkson, J., Jackson, D.M. & Sammut, I.A. (2007) Mitochondrial involvement in transhemispheric diaschisis following hypoxia-ischemia: Clomethiazole-mediated amelioration. *Neuroscience*, **144**, 547–561.
- Elfering, S.L., Sarkela, T.M. & Giulivi, C. (2002) Biochemistry of mitochondrial nitric-oxide synthase. *J. Biol. Chem.*, **277**, 38079–38086.
- Eliasson, M.J., Huang, Z., Ferrante, R.J., Sasamata, M., Molliver, M.E., Snyder, S.H. & Moskowitz, M.A. (1999) Neuronal nitric oxide synthase activation and peroxynitrite formation in ischemic stroke linked to neural damage. *J. Neurosci.*, **19**, 5910–5918.
- Forstermann, U., Schmidt, H.H., Kohlhaas, K.L. & Murad, F. (1992) Induced RAW 264.7 macrophages express soluble and particulate nitric oxide synthase: inhibition by transforming growth factor-beta. *Eur. J. Pharmacol.*, **225**, 161–165.
- Franco, M.C., Arciuch, V.G., Peralta, J.G., Galli, S., Levisman, D., Lopez, L.M., Romorini, L., Poderoso, J.J. & Carreras, M.C. (2006) Hypothyroid phenotype is contributed by mitochondrial complex I inactivation due to translocated neuronal nitric-oxide synthase. *J. Biol. Chem.*, **281**, 4779–4786.
- Ghafoorifar, P., Schenk, U., Klein, S.D. & Richter, C. (1999) Mitochondrial nitric-oxide synthase stimulation causes cytochrome c release from isolated mitochondria. Evidence for intramitochondrial peroxynitrite formation. *J. Biol. Chem.*, **274**, 31185–31188.
- Giulivi, C. (2003) Characterization and function of mitochondrial nitric-oxide synthase. *Free Radic. Biol. Med.*, **34**, 397–408.
- Giulivi, C., Kato, K. & Cooper, C.E. (2006) Nitric oxide regulation of mitochondrial oxygen consumption I: cellular physiology. *Am. J. Physiol. Cell Physiol.*, **291**, C1225–C1231.
- Giulivi, C., Poderoso, J.J. & Boveris, A. (1998) Production of nitric oxide by mitochondria. *J. Biol. Chem.*, **273**, 11038–11043.
- Goss, S.P., Singh, R.J., Hogg, N. & Kalyanaraman, B. (1999) Reactions of *NO, *NO₂ and peroxynitrite in membranes: physiological implications. *Free Radic. Res.*, **31**, 597–606.
- Hamburger, V. (1960) *A Manual of Experimental Embryology*. University of Chicago Press, Chicago, pp. 143–149.
- Han, D., Williams, E. & Cadenas, E. (2001) Mitochondrial respiratory chain-dependent generation of superoxide anion and its release into the intermembrane space. *Biochem. J.*, **353**, 411–416.
- Hattori, I., Takagi, Y., Nozaki, K., Kondo, N., Bai, J., Nakamura, H., Hashimoto, N. & Yodoi, J. (2002) Hypoxia-ischemia induces thioredoxin expression and nitrotyrosine formation in new-born rat brain. *Redox. Rep.*, **7**, 256–259.
- Haynes, V., Elfering, S.L., Squires, R.J., Traaseth, N., Solien, J., Ettl, A. & Giulivi, C. (2003) Mitochondrial nitric-oxide synthase: role in pathophysiology. *IUBMB Life*, **55**, 599–603.
- Kanai, A.J., Pearce, L.L., Clemens, P.R., Birder, L.A., VanBibber, M.M., Choi, S.Y., de Groat, W.C. & Peterson, J. (2001) Identification of a neuronal nitric oxide synthase in isolated cardiac mitochondria using electrochemical detection. *Proc. Natl Acad. Sci. USA*, **98**, 14126–14131.
- Knowles, R.G. & Salter, M. (1998) Measurement of NOS activity by conversion of radiolabeled arginine to citrulline using ion-exchange separation. *Meth. Mol. Biol.*, **100**, 67–73.
- Koeck, T., Fu, X., Hazen, S.L., Crabb, J.W., Stuehr, D.J. & Aulak, K.S. (2004) Rapid and selective oxygen-regulated protein tyrosine denitration and nitration in mitochondria. *J. Biol. Chem.*, **279**, 27257–27262.
- Lacza, Z., Puskar, M., Figueroa, J.P., Zhang, J., Rajapakse, N. & Busija, D.W. (2001) Mitochondrial nitric oxide synthase is constitutively active and is functionally upregulated in hypoxia. *Free Radic. Biol. Med.*, **31**, 1609–1615.
- Lowry, O.H., Rosebrough, N.J., Farr, A.L. & Randall, R.J. (1951) Protein measurement with the Folin phenol reagent. *J. Biol. Chem.*, **193**, 265–275.
- Murray, J., Taylor, S.W., Zhang, B., Ghosh, S. & Capaldi, R.A. (2003) Oxidative damage to mitochondrial complex I due to peroxynitrite: identification of reactive tyrosines by mass spectrometry. *J. Biol. Chem.*, **278**, 37223–37230.
- Pearce, L.L., Kanai, A.J., Epperly, M.W. & Peterson, J. (2005) Nitrosative stress results in irreversible inhibition of purified mitochondrial complexes I and III without modification of cofactors. *Nitric Oxide*, **13**, 254–263.
- Peralta, J.G., Finocchietto, P.V., Converso, D., Schopfer, F., Carreras, M.C. & Poderoso, J.J. (2003) Modulation of mitochondrial nitric oxide synthase and energy expenditure in rats during cold acclimation. *Am. J. Physiol. Heart Circ. Physiol.*, **284**, H2375–H2383.
- Poderoso, J.J., Carreras, M.C., Lisdero, C., Riobo, N., Schopfer, F. & Boveris, A. (1996) Nitric oxide inhibits electron transfer and increases superoxide radical production in rat heart mitochondria and submitochondrial particles. *Arch. Biochem. Biophys.*, **328**, 85–92.
- Pozo Devoto, V.M., Chavez, J.C. & Fiszer de Plazas, S. (2006) Acute hypoxia and programmed cell death in developing CNS: Differential vulnerability of chick optic tectum layers. *Neuroscience*, **142**, 645–653.
- Puka-Sundvall, M., Gajkowska, B., Cholewinski, M., Blomgren, K., Lazarewicz, J.W. & Hagberg, H. (2000a) Subcellular distribution of calcium and ultrastructural changes after cerebral hypoxia-ischemia in immature rats. *Brain Res. Dev. Brain Res.*, **125**, 31–41.
- Puka-Sundvall, M., Wallin, C., Gilland, E., Hallin, U., Wang, X., Sandberg, M., Karlsson, J., Blomgren, K. & Hagberg, H. (2000b) Impairment of mitochondrial respiration after cerebral hypoxia-ischemia in immature rats: relationship to activation of caspase-3 and neuronal injury. *Brain Res. Dev. Brain Res.*, **125**, 43–50.
- Radi, R. (2004) Nitric oxide, oxidants, and protein tyrosine nitration. *Proc. Natl Acad. Sci. USA*, **101**, 4003–4008.
- Reynolds, E.S. (1963) The use of lead citrate at high pH as an electron-opaque stain in electron microscopy. *J. Cell Biol.*, **17**, 208–212.
- Ribatti, D., Nico, B. & Bertossi, M. (1993) The development of the blood-brain barrier in the chick. Studies with Evans blue and horseradish peroxidase. *Ann. Anat.*, **175**, 85–88.
- Riobo, N.A., Clementi, E., Melani, M., Boveris, A., Cadenas, E., Moncada, S. & Poderoso, J.J. (2001) Nitric oxide inhibits mitochondrial NADH: ubiquinone reductase activity through peroxynitrite formation. *Biochem. J.*, **359**, 139–145.
- Rodriguez De Lores Arnaiz, G. & De Robertis, E.D. (1962) Cholinergic and non-cholinergic nerve endings in the rat brain. II. Subcellular localization of monoamine oxidase and succinate dehydrogenase. *J. Neurochem.*, **9**, 503–508.
- Rodriguez Gil, D.J., Viapiano, M.S. & Fiszer de Plazas, S. (2000) Acute hypoxic hypoxia transiently reduces GABA (A) binding site number in developing chick optic lobe. *Brain Res. Dev. Brain Res.*, **124**, 67–72.
- Schild, L., Reinheckel, T., Reiser, M., Horn, T.F., Wolf, G. & Augustin, W. (2003) Nitric oxide produced in rat liver mitochondria causes oxidative stress and impairment of respiration after transient hypoxia. *Faseb J.*, **17**, 2194–2201.
- Solien, J., Haynes, V. & Giulivi, C. (2005) Differential requirements of calcium for oxoglutarate dehydrogenase and mitochondrial nitric-oxide synthase under hypoxia: impact on the regulation of mitochondrial oxygen consumption. *Comp. Biochem. Physiol. a Mol. Integr. Physiol.*, **142**, 111–117.
- Sugawara, T., Fujimura, M., Noshita, N., Kim, G.W., Saito, A., Hayashi, T., Narasimhan, P., Maier, C.M. & Chan, P.H. (2004) Neuronal death/survival signaling pathways in cerebral ischemia. *NeuroRx*, **1**, 17–25. [*J. Am. Soc. Exp. Neurotherapeutics*].
- Tatoyan, A. & Giulivi, C. (1998) Purification and characterization of a nitric-oxide synthase from rat liver mitochondria. *J. Biol. Chem.*, **273**, 11044–11048.
- Turrens, J.F. & Boveris, A. (1980) Generation of superoxide anion by the NADH dehydrogenase of bovine heart mitochondria. *Biochem. J.*, **191**, 421–427.
- Vacotto, M., Paz, D. & de Plazas, S.F. (2006) Hypoxia-induced cell death and activation of pro- and anti-apoptotic proteins in developing chick optic lobe. *Neurochem. Res.*, **31**, 1003–1009.
- Volpe, J.J. (2001) Perinatal brain injury: from pathogenesis to neuroprotection. *Ment. Retard. Dev. Disabil. Res. Rev.*, **7**, 56–64.
- Won, S.J., Kim, D.Y. & Gwag, B.J. (2002) Cellular and molecular pathways of ischemic neuronal death. *J. Biochem. Mol. Biol.*, **35**, 67–86.
- Yamamoto, T., Maruyama, W., Kato, Y., Yi, H., Shamamoto-Nagai, M., Tanaka, M., Sato, Y. & Naoi, M. (2002) Selective nitration of mitochondrial complex I by peroxynitrite: involvement in mitochondria dysfunction and cell death of dopaminergic SH-SY5Y cells. *J. Neural Transm.*, **109**, 1–13.
- Zaborny, T., Valdez, L.B., La Padula, P., Costa, L.E. & Boveris, A. (2005) Effect of sustained hypobaric hypoxia during maturation and aging on rat myocardium. II. mtNOS activity. *J. Appl. Physiol.*, **98**, 2370–2375.
- Zhu, C., Wang, X., Qiu, L., Peeters-Scholte, C., Hagberg, H. & Blomgren, K. (2004) Nitrosylation precedes caspase-3 activation and translocation of apoptosis-inducing factor in neonatal rat cerebral hypoxia-ischaemia. *J. Neurochem.*, **90**, 462–471.
- Zoratti, M. & Szabo, I. (1995) The mitochondrial permeability transition. *Biochim. Biophys. Acta*, **1241**, 139–176.